Smart Structures and Systems, *Vol. 31*, *No. 3* (*2023*) *301-309*
https://doi.org/10.12989/sss.2023.31.3.301

A wireless sensor with data-fusion algorithm for structural tilt measurement

Dan Li [1,2], Guangwei Zhang [2], Ziyang Su [2] and Jian Zhang[*2,3]

[1] *China-Pakistan Belt and Road Joint Laboratory on Smart Disaster Prevention of Major Infrastructures*, *Southeast University*, *Nanjing*, *Jiangsu 211189*, *China*
[2] *School of Civil Engineering*, *Southeast University*, *Nanjing*, *Jiangsu 211189*, *China*
[3] *Jiangsu Key Laboratory of Engineering Mechanics*, *Southeast University*, *Southeast University*, *Nanjing*, *Jiangsu 211189*, *China*

(*Received August 18*, *2022*, *Revised November 10*, *2022*, *Accepted February 28*, *2023*)

Abstract. Tilt is a key indicator of structural safety. Real-time monitoring of tilt responses helps to evaluate structural condition, enable cost-effective maintenance, and enhance lifetime resilience. This paper presents a prototype wireless sensing system for structural tilt measurement. Long range (LoRa) technology is adopted by the sensing system to offer long-range wireless communication with low power consumption. The sensor integrates a gyroscope and an accelerometer as the sensing module. Although tilt can be estimated from the gyroscope or the accelerometer measurements, these estimates suffer from either drift issue or high noise. To address this challenging issue and obtain more reliable tilt results, two sensor fusion algorithms, the complementary filter and the Kalman filter, are investigated to fully exploit the advantages of both gyroscope and accelerometer measurements. Numerical simulation is carried out to validate and compare the sensor fusion algorithms. Laboratory experiment is conducted on a simply supported beam under moving vehicle load to further investigate the performance of the proposed wireless tilt sensing system.

Keywords: complementary filter; data fusion; Kalman filter; structural health monitoring; tilt measurement; wireless sensor

1. Introduction

Structural health monitoring (SHM) is the process of identifying, locating, and quantifying the onset of damages based on analysis of measured responses of engineering structures such as buildings and bridges. Structural tilt is one of the responses that provide critical information regarding the condition of structures (Huang *et al*. 2019). There is a large and ever-growing number of applications for tilt in the field of SHM. Calcaterra *et al*. (2012) evaluated the movements of landslides by means of the inclinometer measurements. Alamdari *et al*. (2019) proposed a bridge condition assessment methodology using rotation influence line at the bridge bearing locations. Huseynov *et al*. (2020) investigated the sensitivity of rotation to various damage scenarios and investigated the effect of sensor location on the sensitivity. Li *et al*. (2020) reconstructed dynamic deflection of high-speed railway bridges using inclination measurements from optimally configured sensors. These successful practices require reliable tilt measurements with high integrity.

Most tilt sensors measure the angle of an object with respect to the direction of gravity through electric effect (Ozioko *et al*. 2021) or magnetic effect (Su *et al*. 2017). Among all these types of sensors, the microelectron-mechanical system (MEMS) based accelerometer has been widely used for tilt measurement due to its advantageous properties including small size, light weight, low cost, and high accuracy (Kok *et al*. 2017). Extensive research has demonstrated that the accelerometer can provide reliable measurement for static tilt responses but encounters difficulties in the dynamic environment (Liu *et al*. 2017). This unsatisfactory result mainly stems from external forces acting on the sensor causing unwanted acceleration measurement.

An alternative device for tilt measurement is the gyroscope which outputs angular velocity of the sensor. Tilt can then be estimated through integration of the gyroscope measurement. Compared to the acceleration data, the gyroscope measurement is less venerable to external forces, and therefore the gyroscope-based estimate can effectively capture the high frequency components in the tilt response. However, since the measurement is inevitably corrupted by bias and noise, integration of the gyroscope measurement leads to a signal which suffers from drift issue.

To overcome the limitation using individual sensor, various data fusion approaches have been developed and investigated for improving the tilt sensing performance. The data fusion approaches aim at finding an optimized tilt estimate given measurements from two or more types of sensors. Liu *et al*. (2017) utilized the Tikohnov regularization approach to form a minimization problem combining the acceleration and angular velocity data, and the problem was solved using the variational method. Kok *et al*. (2014) proposed to obtain the maximum *a posteriori* (MAP) orientation estimate of an object by solving a constrained optimization problem through an infeasible start

*Corresponding author, Ph.D., Professor,
E-mail: jian@seu.edu.cn

ISSN: 1738-1584 (Print), 1738-1991 (Online)

Gauss-Newton method. Although the optimization-based approaches provide stable and accurate tilt estimate, the computational complexity and non-causal feature limit the application of these approaches.

Alternatively, the data fusion problem can be solved by filtering approaches which estimate tilt at time t based on measurements up to time t. Among the filtering approaches, the complementary filter and the Kalman filter are pervasive in the areas of orientation estimation (Ladetto 2000, St-Pierre and Gingras 2004, Kottath *et al*. 2017). Consisting of a low-pass filter and a high-pass filter, the complementary filter combines the low frequency components of the acceleration-based tilt estimate and the high frequency components of the gyroscope-based tilt estimate to form a more reliable signal. The complementary filter can effectively relieve both the noise and drift issue. As a simple but effective approach, the complementary filter requires little computational effort, which is desirable for embedded systems. On the other hand, the Kalman filter computes *a posteriori* probabilistic estimates of unknown state variables based on system equations and noisy measurements. Based on Gaussian assumption, the Kalman filter has solid mathematical foundations and achieves the best linear unbiased estimate in the minimum mean-square-error sense (Arunshankar 2020). Compared to the complementary filter, the Kalman filter is more computationally demanding but offers additional design flexibility resulting in better estimation accuracy in most cases (Nowicki *et al*. 2015). Although both the complementary filter and the Kalman filter have been extensively studied for navigation purposes, these filtering approaches are seldom reported for SHM applications of civil structures, and more research is needed to investigate their performance of estimating structural tilt with small magnitude.

To meet the requirements of SHM applications, research efforts have been devoted into developing structural tilt sensor platforms. Faulkner *et al*. (2020) developed a data acquisition (DAQ) system configured to operate with a triaxial accelerometer and two uniaxial gyroscopes for structural tilt measurement. The proposed sensing system was tested experimentally on a single-span skewed railway bridge under traffic loading. Although promising measurement results can be obtained, the high time consumption associated with installation of the complicated DAQ system is among various factors that hinder the large-scale deployment of the sensing system. Testoni *et al*. (2019) designed a tilt sensor deployed with the complementary filter for vibration-based SHM. The proposed sensor works well in both static and dynamic environments, but the cabled data acquisition system limits the application of the sensor. With the advance of wireless communication technology, wireless sensing systems have been developed for SHM application for faster installation process and lower system cost (Shen *et al*. 2021, Fu *et al*. 2021). For structural tilt measurement, Ha *et al*. (2013) proposed a wireless tilt sensor node consisting of two single-axis accelerometer-based inclinometers which can effectively capture static or low-frequency tilt responses. However, the sensor performance in dynamic tilt measurement has not been verified.

This research proposes a wireless tilt sensing system implemented with the sensor fusion algorithm that provides reliable structural tilt measurements with high integrity. The prototype wireless sensor exploits MEMS and wireless technology leading to a low-cost and miniaturized solution capable of collecting tilt data and wirelessly transmitting data. A STMicroelectronics microcontroller is adopted in the wireless tilt sensor to manage the collected data and implement the sensor fusion algorithms. The sensor incorporates a wireless module featuring the Long Range (LoRa) technology for reliable wireless communication. The sensing module integrates a gyroscope and an accelerometer to provide response measurement data for structural tilt estimation. This research compares and discusses the data fusion performance of the complementary filter and the Kalman filter through numerical simulation of a simply supported beam structure under moving load. Following the discussion, a laboratory tilt measurement experiment is conducted to investigate the reliability of the proposed wireless sensor.

The rest of this paper is organized as follows. Section 2 introduces the hardware design of the wireless tilt sensor and describes functional modules for computing core, wireless communication, and response sensing. Section 3 covers the tilt sensing approaches, emphasizing the fusion algorithms that combine gyroscope data and acceleration data. Numerical simulation of the sensor fusion is presented in Section 4, and experimental validation of the designed wireless sensor is discussed in Section 5. In the end, Section 6 closes the paper with conclusion and future work.

2. Wireless sensor design

This section introduces the design of wireless tilt sensor. As shown in Fig. 1, the wireless sensing node consists of three functional modules: embedded computational core, wireless communication module, and motion sensing module. Details of these three modules are described as follows.

2.1 Embedded computational core

The wireless sensing node adopts a STMicroelectronics microcontroller (STM32F103RCT6) as the host processor to execute tasks of data acquisition and onboard computing. Based on the high-performance ARM® Cortex®-M3 32-bit RISC core, the STM32F103RCT6 operates at a 72 MHz maximum frequency. This microcontroller contains 256 KB reprogrammable flash memory for storing the embedded software and 48 KB static random-access memory (SRAM) for storing stack and heap variables. The STM32F103RCT6 offers a wide variety of advanced communication interfaces, including three Serial Peripheral Interfaces (SPIs), two Inter-Integrated Circuits (I2Cs), two Inter-Integrated Sounds (I2Ss), one Secure Digital Input Output (SDIO), one Controller Area Network (CAN) port, one Universal Serial Bus (USB) port, and five Universal Synchronous/Asynchronous Receive Transmitters (USRATs).

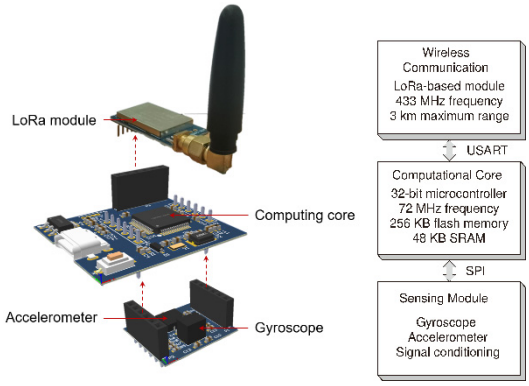

Fig. 1 Functional diagram of wireless sensing node hardware design

These interfaces enable the microcontroller to communicate with other hardware devices. The employed timer and interrupt modules allow for the design of precise timing applications, such as sampling sensor data at specified frequencies.

The selection of the STM32F103RCT6 as host processor is to balance power consumption versus computational functionality. Running at 72 MHz, the microcontroller consumes about 40 mA with necessary peripherals enabled. Considering this active-mode power consumption, normal batteries available in the market can easily support the microcontroller operating for days. The STM32F103RCT6 also supports a comprehensive set of low-power modes. With suitable software configuration interleaving active and sleep modes, the microcontroller could operate for a much longer time before onboard power supply runs out.

2.2 Wireless communication module

The wireless communication module servers as the interface for data exchange between sensing nodes and data server. Sufficient communication reliability, range, and data transfer rate are needed for wireless SHM network.

In this prototype sensing system, each sensing node has a wireless communication module based on Semtech SX1278. The module is interfaced with the microcontroller through a USART for exchanging data and radio commands. The SX1278 features the LoRa long range modem which enables long range data transmissions and high inference immunity with low power consumption. LoRa is developed for supporting the Low Power Wide Area Network (LPWAN) and operates on license-free sub-gigahertz radio frequency for wireless communication. Based on a chirp spread spectrum (CSS) modulation, LoRa encodes information using frequency chirps with a linear variation of frequency over time. This improves robustness of wireless communication in case of multipath propagation interferences.

Compared to other widely used wireless technologies like cellular, WiFi, Bluetooth, or ZigBee, LoRa provides a significantly greater communication range while us3ng minimal power, which is desirable for SHM applications (Augustin *et al*. 2016).

Table 1 Key parameters of the wireless module

Parameter	Value
Operating frequency	410 ~ 441 MHz
Data transfer rate	19.2 kbps
Maximum range	about 3 km
Transmitting power consumption	118 mA

The key parameters of the wireless communication module are summarized in Table 1. The LoRa-based module is selected to balance low power consumption required for wireless sensing and long communication range typically needed for monitoring civil structures.

2.3 Motion sensing module

To obtain motion measurements, the sensing module consists of a gyroscope ADXRS290 and an accelerometer ADXL355. The selected sensing devices feature low noise density, low offset drift, and low power consumption which are desirable for SHM application in the presence of vibration. Both sensors are MEMS-based devices which convert mechanical signals into electric voltages. The generated analog signals are fed into the internal low-pass filter for noise reduction. The filtered signals are then digitized by the analog-to-digital converters (ADCs) inside the sensors. The built-in signal conditioner and ADCs offer guaranteed measurement accuracy while minimizing the effort and expense associated with compensation and calibration. For structural tilt measurements, the full-scale ranges of gyroscope and accelerometer are set to as $\pm 100\,°/s$ and $\pm 2\,g$, respectively. Both sensors are communicated with the microcontroller through the SPI digital interface for data transmission and sensor setting.

3. Sensor fusion algorithm

3.1 Gyroscope-based tilt estimation

A gyroscope measures the angular velocity about the x, y, and z axes of the sensor body frame, denoted as ω_x, ω_y, and ω_z, respectively. Fig. 2 illustrates the relationship between Euler angle rates and body frame axis rates.

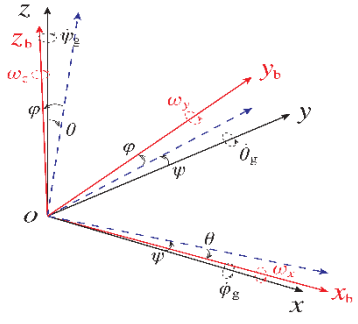

Fig. 2 Schematic of Euler angle rates and body frame axis rates

According to kinematics of moving frame, the rate of Euler angles can be determined by the gyroscope measurements

$$\begin{pmatrix}\dot{\phi}_{\mathrm{g}}\\ \dot{\theta}_{\mathrm{g}}\\ \dot{\psi}_{\mathrm{g}}\end{pmatrix}=\begin{pmatrix}1 & \sin\phi\tan\theta & \cos\phi\tan\theta\\ 0 & \cos\phi & -\sin\phi\\ 0 & -\sin\phi/\cos\theta & \cos\phi/\cos\theta\end{pmatrix}\begin{pmatrix}\omega_x\\ \omega_y\\ \omega_z\end{pmatrix} \quad (1)$$

For SHM applications, structural tilt magnitude is typically close to zero, and thus the rate of Euler angles can be effectively approximated by the body-referenced angular velocity

$$\dot{\phi}_{\mathrm{g}}\approx\omega_x,\quad \dot{\theta}_{\mathrm{g}}\approx\omega_y,\quad \dot{\psi}_{\mathrm{g}}\approx\omega_z \quad (2)$$

If the gyroscope measurements were perfect, accurate tilt responses could be calculated by integrating the rate of Euler angles over time. In practice, however, gyroscope measurements are always corrupted by a bias $\boldsymbol{\delta}_{\mathrm{g}}$ and noise $\boldsymbol{e}_{\mathrm{g}}$ which introduce drift in the integration process. The gyroscope measurement model is given by

$$\boldsymbol{\omega}=\boldsymbol{\omega}_{\mathrm{true}}+\boldsymbol{\delta}_{\mathrm{g}}+\boldsymbol{e}_{\mathrm{g}} \quad (3)$$

To compensate the drift issue, the tilt estimates from the gyroscope data need to be supplemented with other types of sensors such as accelerometer.

3.2 Accelerometer-based tilt estimation

An accelerometer measures the acceleration in the sensor body frame. In the absence of external force, the accelerometer outputs are projections of the gravity on the three sensing axes and can be used to determine the rotation angles (as shown in Fig. 3). In this scenario, the accelerometer measurements are given as

$$\begin{pmatrix}a_x\\ a_y\\ a_z\end{pmatrix}=\begin{pmatrix}-\sin\theta\\ \cos\theta\sin\phi\\ \cos\theta\cos\phi\end{pmatrix}g=\boldsymbol{R}g \quad (4)$$

According to Eq. (4), the structural tilt angles can be estimated using acceleration data

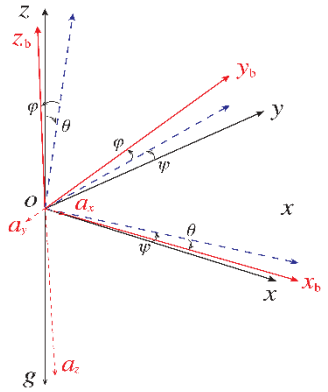

Fig. 3 Accelerometer-based tilt estimation

$$\phi_{\mathrm{a}}=\arctan\left(\frac{a_y}{a_z}\right)$$
$$\theta_{\mathrm{a}}=\arctan\left(-\frac{a_x}{\sqrt{a_y^2+a_z^2}}\right) \quad (5)$$

Similar to the gyroscope, the accelerometer measurements are typically corrupted by a bias and intrinsic noise. In addition, an accelerometer outputs both gravity and linear acceleration caused by external force. Since in practice the accelerometer measurements are typically dominated by the gravity (Kok *et al.* 2017), the linear acceleration can be modeled as noise source disturbing the tilt measurement. With all these effects taken into account, the acceleration measurement model is usually given by

$$\boldsymbol{a}=\boldsymbol{R}g+\boldsymbol{\delta}_{\mathrm{a}}+\boldsymbol{e}_{\mathrm{a}} \quad (6)$$

where $\boldsymbol{\delta}_{\mathrm{a}}$ denotes the bias of the accelerometer and $\boldsymbol{e}_{\mathrm{a}}$ denotes the sensor noise. Note that the noise term $\boldsymbol{e}_{\mathrm{a}}$ in this model does not only represent the sensor noise, but also includes the modeling uncertainty induced by the linear acceleration.

3.3 Complementary filter

The complementary filter combines measurements of the gyroscope and accelerometer to provide more reliable tilt estimate. It has been found that the gyroscope-based tilt estimate is accurate on a short term but drifts over time, while the accelerometer-based tilt estimate is susceptible to external disturbance but desirable on a long time scale. The complementary filter exploits these properties, and implements a low-pass filter $L(s)$ on the tilt estimate using accelerometer data and a high-pass filter $H(s)=1-L(s)$ on the tilt estimate using gyroscope data. Since the sum of the low-pass filter and high-pass filter equals to unity over the entire frequency range, the fusion of the two types of sensor data provides an all-pass estimate of tilt.

Taking the pitch angle θ estimation as an example, the complementary filtering process is illustrated in Fig. 4. The output of the complementary filter is given as

$$\Theta_{\mathrm{cf}}(s)=H(s)\left(\frac{1}{s}\Omega_y(s)\right)+L(s)\Theta_{\mathrm{a}}(s) \quad (7)$$

where $\Theta_{\mathrm{cf}}(s)$, $\Theta_{\mathrm{a}}(s)$, and $\Omega_y(s)$ are the Laplace transforms of the filtered angle θ_{cf}, the accelerometer-based estimate θ_{a}, and the gyroscope measurement ω_y, respectively. Utilizing the first-order filters $L(s)=f_{\mathrm{c}}/(s+f_{\mathrm{c}})$ and $H(s)=s/(s+f_{\mathrm{c}})$ with cut-off frequency as f_{c}, the complementary filtering system can be digitized as

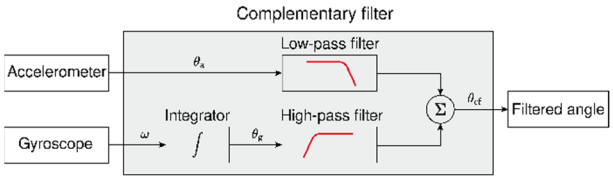

Fig. 4 Schematic of the complementary filtering process

$$\theta_{\mathrm{cf},k} = \gamma\left(\theta_{\mathrm{cf},k-1} + \omega_{y,k}\Delta t\right) + (1-\gamma)\theta_{\mathrm{a},k} \tag{8}$$

Here $\gamma = \tau/(\tau + \Delta t)$ is the control coefficient for the filter where $\tau = 1/f_c$ is the time constant and Δt is the sampling period of both sensors. The performance of complementary filter largely depends on the cut-off frequency f_c, which defines the boundary between trusting the gyroscope and trusting the accelerometer. With a lower cut-off frequency, the gyroscope data take priority over accelerometer data; conversely, a filter with higher cut-off frequency puts more weight on tilt estimate obtained from the accelerometer measurement. Although higher order complementary filters have been proposed for specific applications (Liu *et al*. 2017, Narkhede *et al*. 2019), the simple form Eq. (8) has been proven to be effective and widely used for tilt estimation (Gui *et al*. 2015).

3.4 Kalman filter

An alternative to using complementary filter for tilt estimation is to use the Kalman filter. As a Bayesian approach, Kalman filter produces *a posteriori* probabilistic estimates of unknown state based on system equation and noisy measurements. Consider a linear discrete-time system with additive noises

$$\begin{aligned} &\text{process:} && \boldsymbol{x}_k = \boldsymbol{A}_{k-1}\boldsymbol{x}_{k-1} + \boldsymbol{B}_{k-1}\boldsymbol{u}_{k-1} + \boldsymbol{w}_{k-1} \\ &\text{measurement:} && \boldsymbol{y}_k = \boldsymbol{C}_k\boldsymbol{x}_k + \boldsymbol{v}_k \end{aligned} \tag{9}$$

Here $\boldsymbol{u}_{k-1}$ is a known input to the system. The process noise $\boldsymbol{w}_{k-1}$ and measurement noise $\boldsymbol{v}_k$ are mutually independent, zero-mean Gaussian processes with covariance matrices $\boldsymbol{\Sigma}_{\boldsymbol{w}}$ and $\boldsymbol{\Sigma}_{\boldsymbol{v}}$, respectively.

The Kalman filter recursively updates the state $\boldsymbol{x}$ from measurements $\boldsymbol{y}$ through a two-step procedure. In the time update step, the state and corresponding covariance matrix are propagated through the system equation

$$\begin{aligned} \widehat{\boldsymbol{x}}_{k|k-1} &= \boldsymbol{A}_{k-1}\widehat{\boldsymbol{x}}_{k-1|k-1} + \boldsymbol{B}_{k-1}\boldsymbol{u}_{k-1} \\ \boldsymbol{\Sigma}_{\boldsymbol{x},k|k-1} &= \boldsymbol{A}_{k-1}\boldsymbol{\Sigma}_{\boldsymbol{x},k-1|k-1}\boldsymbol{A}_{k-1}^{\mathrm{T}} + \boldsymbol{\Sigma}_{\boldsymbol{w}} \end{aligned} \tag{10}$$

In the measurement update step, the Kalman gain matrix $\boldsymbol{K}_k$ is evaluated to minimize the trace of the *a posteriori* covariance matrix

$$\boldsymbol{K}_k = \boldsymbol{\Sigma}_{\boldsymbol{x},k|k-1}\boldsymbol{C}_k^{\mathrm{T}}\left(\boldsymbol{C}_k\boldsymbol{\Sigma}_{\boldsymbol{x},k|k-1}\boldsymbol{C}_k^{\mathrm{T}} + \boldsymbol{\Sigma}_{\boldsymbol{v}}\right)^{-1} \tag{11}$$

Upon availability of the measurement $\boldsymbol{y}_k$, the *a posteriori* estimate $\widehat{\boldsymbol{x}}_{k|k}$ and corresponding covariance matrix $\boldsymbol{\Sigma}_{\boldsymbol{x},k|k}$ can be calculated as

$$\begin{aligned} \widehat{\boldsymbol{x}}_{k|k} &= \widehat{\boldsymbol{x}}_{k|k-1} + \boldsymbol{K}_k\left(\boldsymbol{y}_k - \boldsymbol{C}_k\widehat{\boldsymbol{x}}_{k|k-1}\right) \\ \boldsymbol{\Sigma}_{\boldsymbol{x},k|k-1} &= (\boldsymbol{I} - \boldsymbol{K}_k\boldsymbol{C}_k)\boldsymbol{\Sigma}_{\boldsymbol{x},k|k-1} \end{aligned} \tag{12}$$

3.4.1 Connection to the complementary filter

Although Section 3.3 derives the complementary filter by analysis in frequency domain, it turns out that the complementary filter can be interpreted as a steady-state Kalman filter (Higgins 1975). To highlight this relationship, the recursive updating process Eq. (8) can be equivalently decomposed into two steps

$$\begin{aligned} \theta_{\mathrm{cf},k|k-1} &= \theta_{\mathrm{cf},k-1|k-1} + \omega_{y,k}\Delta t \\ \theta_{\mathrm{cf},k|k} &= \theta_{\mathrm{cf},k|k-1} + (1-\gamma)\left(\theta_{\mathrm{a},k} - \theta_{\mathrm{cf},k|k-1}\right) \end{aligned} \tag{13}$$

Here the system input is the gyroscope measurement $\omega_{y,k}$, and the system measurement is the tilt estimate from accelerometer data $\theta_{\mathrm{a},k}$. Comparing Eq. (13) with Eq. (12), the Kalman gain can be obtained as $K = 1 - \gamma$.

On the other hand, the steady-state Kalman gain can be determined by substituting the steady-state covariance for the *a priori* covariance in Eq. (11). The steady-state covariance can be obtained by solving the discrete-time algebraic Riccati equation (DARE) (Simon 2006). For the tilt estimation system Eq. (13), all quantities are time-invariant scalars such that $A = 1$, $B = \Delta t$, and $C = 1$. The solution to the resulting DARE is calculated as

$$\Sigma_{\theta,\infty} = \frac{\Sigma_w + \sqrt{\Sigma_w^2 + 4\Sigma_w\Sigma_v}}{2} \tag{14}$$

The steady-state Kalman gain is obtained as

$$K_\infty = \frac{\Sigma_{\theta,\infty}}{\Sigma_{\theta,\infty} + \Sigma_v} = \frac{2}{1 + \sqrt{1 + \frac{4\Sigma_v}{\Sigma_w}}} \tag{15}$$

For tilt estimation through sensor fusion, the measurement noise covariance Σ_v is usually much larger than the process noise covariance Σ_w, which mainly comes from the gyroscope measurement noise and is attenuated by the integration process.

3.4.2 Gyroscope bias estimation

Although they produce fairly good tilt estimates, the complementary filter and the steady-state Kalman filter simply consider the gyroscope bias to be part of process noise, which may lead to biased estimate in the dynamic motion conditions (Mahony *et al*. 2008, Narkhede *et al*. 2021). To address this issue, the Kalman filter can be extended to include estimation of the gyroscope bias. With the system state $\boldsymbol{x} = \left(\theta, \delta_{\mathrm{g},y}\right)^{\mathrm{T}}$ and input $u = \omega_y$, the process equation is given by

$$\begin{aligned} \boldsymbol{x}_k &= \boldsymbol{A}\boldsymbol{x}_{k-1} + \boldsymbol{B}u_{k-1} + \boldsymbol{w}_{k-1} \\ \begin{pmatrix}\theta \\ \delta_{\mathrm{g},y}\end{pmatrix}_k &= \begin{pmatrix}1 & -\Delta t \\ 0 & 1\end{pmatrix}\begin{pmatrix}\theta \\ \delta_{\mathrm{g},y}\end{pmatrix}_{k-1} + \begin{pmatrix}\Delta t \\ 0\end{pmatrix}\omega_{y,k-1} + \begin{pmatrix}w_\theta \\ w_\delta\end{pmatrix} \end{aligned} \tag{16}$$

The accelerometer-based tilt estimate is still treated as measurement $y = \theta_{\mathrm{a}}$ and the measurement matrix is given by

$$\begin{aligned} y_k &= \boldsymbol{C}\boldsymbol{x}_k + v_k \\ \theta_{\mathrm{a},k} &= \begin{pmatrix}1 & 0\end{pmatrix}\begin{pmatrix}\theta \\ \delta_{\mathrm{g},y}\end{pmatrix}_k + v_\theta \end{aligned} \tag{17}$$

Following Eqs. (10)~(12), both the tilt angle θ and the gyroscope bias $\delta_{\mathrm{g},y}$ can be recursively updated. In order to avoid ambiguity, the Kalman filter in subsequent discussion refers to the formulation with gyroscope bias estimation.

Table 2 Properties of the simply supported bridge

Property	Value
Length (m)	6
Width (mm)	30
Height (mm)	8
Elastic modulus (MPa)	6,000
Mass density (kg/m^3)	500

4. Numerical simulation

To investigate the performance of sensor fusion algorithms for tilt estimation, numerical simulation is performed on a simply supported bridge structure, given properties listed in Table 2.

The numerical model is built to simulate dynamic behavior of a timber beam structure, whose tilt response at the bearing is similar to typical tilt value of a real structure. As shown in Fig. 5, the bridge is modeled as an Euler–Bernoulli beam carrying vehicle load, and a hypothetical sensor is placed at the roller support to measure the dynamic responses of the beam. To reduce computational efforts while capturing essential dynamic characteristics, the bridge-vehicle interaction is not considered, but concentrated forces with moving speed of $v = 0.2$ m/s are modeled instead. At time $t = k\Delta t$, a horizontal force $f_{x,k}$ and a vertical force $f_{y,k}$ are applied to the beam at $x_t = vt$ with the values of

$$\begin{aligned} f_{x,k} &= \xi_x \qquad \xi_x \sim \mathcal{N}(0, 0.01p) \\ f_{y,k} &= p + \xi_y \qquad \xi_y \sim \mathcal{N}(0, 0.01p) \end{aligned} \tag{18}$$

where $p = 245.25$ N is weight of the vehicle; ξ_x and ξ_y are zero-mean white Gaussian noises.

In addition, to consider the energy-dissipating mechanisms, a Rayleigh damping matrix is constructed such that the damping ratio is 5% for the first and second modes. Based on the built model, the dynamical responses of the beam structure are calculated through Newmark-beta method with time step $\Delta t = 0.01$ s.

Based on the simulated dynamic tilt angle, linear acceleration, and angular rate, the accelerometer and gyroscope readings can be generated with measurement noise taken into account. The noise density of the gyroscope is set as $0.01\ °/s/\sqrt{\text{Hz}}$ and a constant bias of $-0.01\ °/s$ is also considered. The noise density of the accelerometer is set as $100\ \mu g/\sqrt{\text{Hz}}$. The simulated gravity is set as 9.82 m/s^2. Fig. 6 plots simulated sensor readings for the loads moving across the beam. It can be observed from Fig.

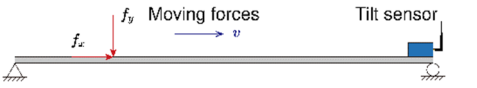

Fig. 5 Simply supported bridge structure model

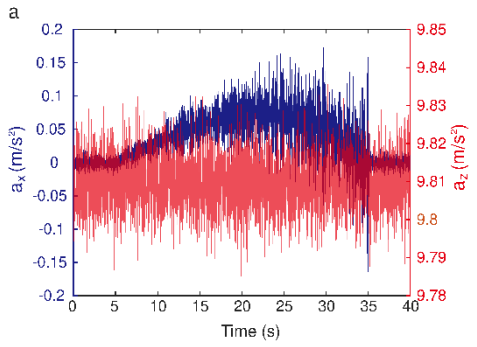

(a) Acceleration measurements

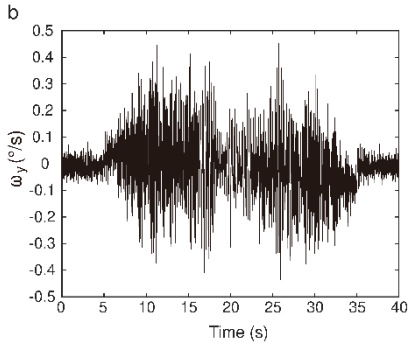

(b) Angular rate measurements

Fig. 6 Simulated sensor readings

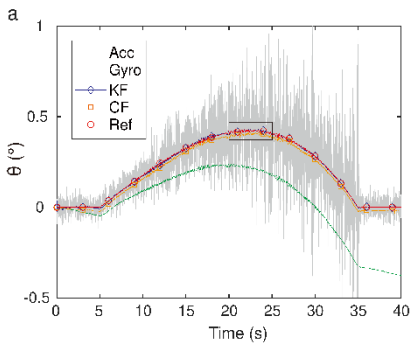

(a) Entire time span

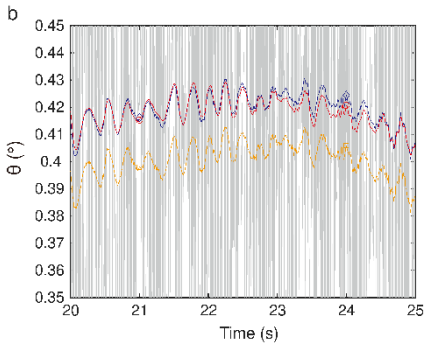

(b) Close-up (20 ~ 25 s)

Fig. 7 Comparison of tilt estimates using simulated data

6(a) that acceleration measurement a_x shows a roughly parabolic shape and acceleration measurement a_z is dominated by the gravity. The measured angular rate ω_y oscillates around0 °/s, as shown in Fig. 6(b).

Given the simulated sensor measurements, tilt at the roller support can be estimated using approaches presented in Section 3. The filter parameters are determined according to the sensor noise level and simulation results. Considering the dynamics of the structure and referring to other work with similar test setup (Huseynov *et al*. 2020), the time constant in the complementary filter is set as $\tau = 2$ s, resulting in the control coefficient as $\gamma = 0.995$. For the Kalman filter, it should be noted that the covariance matrices represent not only the sensor noise, but also the model uncertainty. The process noise covariance is set as $\boldsymbol{\Sigma_w} = \mathrm{diag}(5 \times 10^{-3}(°)^2,\ 10^{-4}(°/\mathrm{s})^2)$; the measurement noise covariance is empirically set as $\Sigma_v = 0.15(°)^2$, which is higher than the noise level of the observed signal to deal with the model uncertainty (Simon 2006) and improve the filter stability (Boutayeb *et al*. 1997).

Fig. 7 plots the tilt estimates results using simulated data. The tilt estimate θ_{a} obtained from the accelerometer measurements is contaminated by considerable noise and the tilt estimate θ_{g} obtained from the gyroscope measurements suffers from drift issue. Both the complementary filter and the Kalman filter can improve the quality of the tilt estimate. Based on current settings, the complementary filter cannot fully resolve the drift issue and the tilt estimate θ_{cf} slightly deviates from the ground truth reference tilt response θ_{ref}. In the Kalman filter, the bias is considered as part of the unknown system states to be recovered, and the resulting tilt estimate θ_{kf} matches well with the reference tilt response.

To quantitatively evaluate the performance of the approaches, the ratio of the root-mean-square-error (RMSE) of the tilt estimation θ_{est} to the largest absolute value of the tilt reference θ_{ref} (Liu *et al*. 2017) is calculated as

$$\text{RMSE ratio} = \frac{\sqrt{\frac{1}{N}\sum_{k=1}^{N}\left(\theta_{\mathrm{ref},k} - \theta_{\mathrm{est},k}\right)^2}}{\max\left(\left|\theta_{\mathrm{ref},k}\right|\right)} \tag{19}$$

where N is the total number of tilt data. The accelerometer-based tilt estimate and the gyroscope-based tilt estimate give a 35.50% RMSE ratio and a 49.71% RMSE ratio, respectively. On the other hand, the complementary filter and the Kalman filter can significantly reduce the RMSE ratio, resulting in a 4.29% error and a 0.83% error, respectively.

5. Experimental validation

A laboratory experiment is conducted on a simply supported timber beam structure to further validate the proposed wireless sensor for structural tilt measurement. Same as the numerical model, the total length of the beam structure is 6 m and dimensions of the cross-section are 30 mm × 8 mm. The structure is oriented such that the beam bends about the weak axis. The beam is placed on two rectangular plates supported by steel cylinders. At one end, the steel cylinder is constrained along longitudinal direction and the support acts as a pinned support; at the other end, the steel cylinder is free to move along longitudinal direction and the support acts as a roller support. In addition, two auxiliary beams with length of 1 m are assembled at the two ends of the structure, respectively.

To emulate tilt behavior of a real bridge under live load, a two-axle model vehicle is pulled through the beam structure at speed of about $v = 0.2$ m/s. Measured by an electronic scale, the total mass of the model vehicle together with the additional mass blocks is about 40 kg. The model vehicle travels along wood rails on the top surface of the beam generating dynamic tilt response at the support.

At the roller support, the designed wireless sensor and a high-precision cabled inclinometer (HWT905, WitMotion) are installed to capture the dynamic behaviors of the beam structure. Triaxial accelerations and biaxial angular rates are collected by the wireless sensor for structural tilt estimation which is compared to the cabled inclinometer output. The sampling frequency of all the measurements is set as 100 Hz. The experiment setup is shown in Fig. 8.

Considering similar sensor and structure dynamics, the wireless sensor adopts the same filter settings as those used

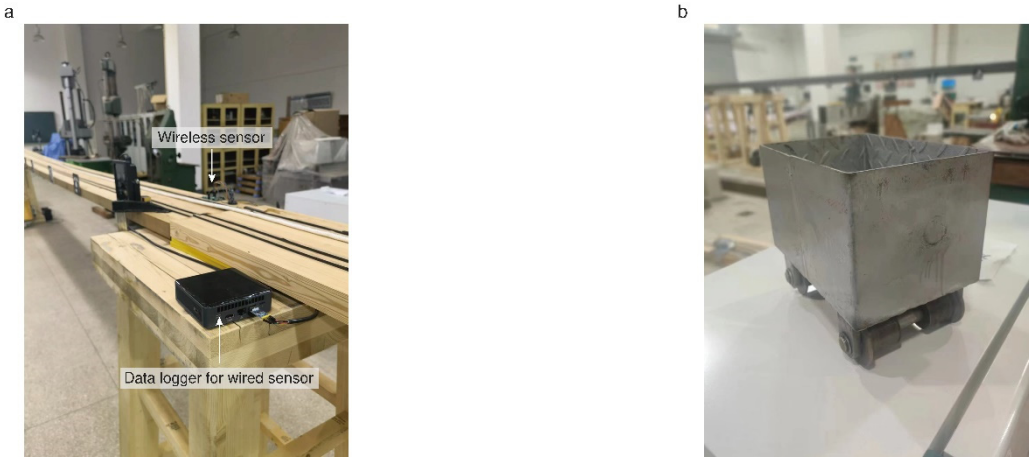

(a) Timber beam structure (b) Model vehichle

Fig. 8 Experiment setup

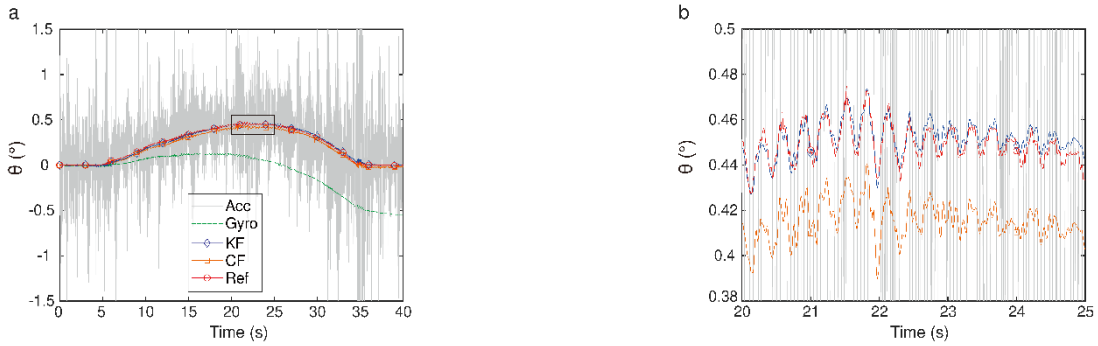

(a) Entire time span (b) Close-up (20 ~ 25 s)

Fig. 9 Comparison of tilt estimates using experimental data

in the simulation. For the complementary filter, the control coefficient is set as $\gamma = 0.995$; for the Kalman filter, the process noise covariance is set as $\boldsymbol{\Sigma_w} = \text{diag}(5 \times 10^{-3}(°)^2, 10^{-4}(°/s)^2)$ and the measurement noise covariance is set as $\Sigma_v = 0.15\ (°)^2$. It should be noted that this specific set of filter parameters may not work for other structures, and need to be calibrated for effective measurement. The dynamic tilt responses obtained by different approaches are displayed in Fig. 9. Similar to the simulated results, the accelerometer-based tilt estimate is highly affected by translational vibration, and the gyroscope-based tilt estimate drifts over time as errors in measurements accumulate during the integration process. From the comparison, it can be seen that the Kalman filter outperforms the complementary filter. By effectively compensating the gyroscope bias, the Kalman filter gives reasonably good tilt estimate which matches well with the reference tilt. The resulting RMSE ratio is calculated as 2.50%. On the other hand, the complementary filter can partially resolve the drift issue and the resulted tilt estimate shows lower accuracy with the RMSE ratio of 5.81%.

6. Conclusions

In this paper, a wireless tilt sensor is designed and validated for SHM applications. The wireless sensor consists of an embedded computational core, a wireless communication module, and a sensing module. As a computational core, the high-performance microcontroller is a powerful component that allows real-time execution of data acquisition and data processing. The sensor adopts the LoRa-based wireless module, balancing the conflict between the requirement for long-distance communication and the requirement for low power consumption. The combination of the MEMS gyroscope and accelerometer, two of the key parts of a wireless sensor, serves as the sensing module.

Structural tilt can be estimated by integrating the angular rate measured using the gyroscope or through the accelerometer outputs which are projections of the gravity. However, it has been shown that neither the gyroscope nor the accelerometer can provide reliable tilt measurement individually. The gyroscope-based tilt estimate is accurate on a short timescale but suffers from integration drift, while the accelerometer-based tilt estimate is accurate over a longer timescale but has a large variance.

Sensor fusion algorithms are implemented to improve tilt sensing performance by combining the information from two sensors. These algorithms include the complementary filter and the Kalman filter. Similarity and difference between these two algorithms have been discussed. Simulation on a simply supported beam structure demonstrates that the Kalman filter is more robust, since it effectively removes the gyroscope bias effect. The proposed sensing system is further validated through laboratory experiment. The wireless sensor measures structural tilt based on acceleration and angular rate responses. The experimental results show that with the Kalman filter implemented, the wireless measured structural tilt has reasonably good agreement with the output of a high-precision cabled inclinometer.

It is noteworthy that besides the sensor fusion algorithms, the sensor quality also plays a critical role in achieving the desired measurement performance. Since structural tilt and angular rate are usually of small magnitude, it is important to select sensors with low noise so that the structural responses can be measured with a sufficiently high level of accuracy.

While the proposed wireless tilt sensor demonstrates promising performance, there is still room for improvement towards deployment of the sensing system for larger structures. Further discussion will be conducted on the effect of low-frequency noise in acceleration measurement. In addition, more systematic studies are needed to investigate the influence of filter parameters on the data fusion performance. Future research will continue to improve the prototype system for greater communication range, low power consumption, and wider application to other civil structures.

Acknowledgments

The authors wish to express appreciations for the funding support of this research from the Jiangsu Provincial Double-Innovation Doctoral Program (No. JSSCBS20210086). Any opinions, findings, and conclusions or recommendations expressed in this publication are those of the author and do not necessarily reflect the view of the

sponsors.

References

Alamdari, M.M., Kildashti, K., Samali, B. and Goudarzi, H.V. (2019), "Damage diagnosis in bridge structures using rotation influence line: Validation on a cable-stayed bridge", *Eng. Struct.*, **185**, 1-14. https://doi.org/10.1016/j.engstruct.2019.01.124

Arunshankar, J. (2020), "Investigations on state estimation of smart structure systems", *Smart Struct. Syst., Int. J.*, **25**(1), 37-45. https://doi.org/10.12989/sss.2020.25.1.037

Augustin, A., Yi, J., Clausen, T. and Townsley, W.M. (2016), "A study of LoRa: Long range & low power networks for the internet of things", *Sensors*, **16**(9), 1466. https://doi.org/10.3390/s16091466

Boutayeb, M., Rafaralahy, H. and Darouach, M. (1997), "Convergence analysis of the extended Kalman filter used as an observer for nonlinear deterministic discrete-time systems", *IEEE Transact. Automat. Control*, **42**(4), 581-586. https://doi.org/10.1109/9.566674

Calcaterra, S., Cesi, C., Di Maio, C., Gambino, P., Merli, K., Vallario, M. and Vassallo, R. (2012), "Surface displacements of two landslides evaluated by GPS and inclinometer systems: A case study in Southern Apennines, Italy", *Natural Hazards*, **61**(1), 257-266. https://doi.org/10.1007/s11069-010-9633-3

Faulkner, K., Brownjohn, J.M.W., Wang, Y. and Huseynov, F. (2020), "Tracking bridge tilt behaviour using sensor fusion techniques", *J. Civil Struct. Health Monitor.*, **10**(4), 543-555. https://doi.org/10.1007/s13349-020-00400-9

Fu, Y., Hoang, T., Mechitov, K., Kim, J.R., Zhang, D. and Spencer, B.F.J. (2021), "xShake: Intelligent wireless system for cost-effective real-time seismic monitoring of civil infrastructure", *Smart Struct. Syst., Int. J.*, **28**(4), 483-497. https://doi.org/10.12989/sss.2021.28.4.483

Gui, P., Tang, L. and Mukhopadhyay, S. (2015), "MEMS based IMU for tilting measurement: Comparison of complementary and kalman filter based data fusion", *Proceedings of 2015 IEEE 10th Conference on Industrial Electronics and Applications* (*ICIEA*), Auckland, New Zealand, June.

Ha, D.W., Park, H.S., Choi, S.W. and Kim, Y.S. (2013), "A wireless MEMS-based inclinometer sensor node for structural health monitoring", *Sensors*, **13**(12), 16090-16104. https://doi.org/10.3390/s131216090

Higgins, W.T. (1975), "A comparison of complementary and Kalman filtering", *IEEE Transact. Aerosp. Electron. Syst.*, **3**, 321-325. https://doi.org/10.1109/TAES.1975.308081

Huang, H., Xie, X., Zhang, D., Liu, Z. and Lacasse, S. (2019), "Multi-sensor data fusion based assessment on shield tunnel safety", *Smart Struct. Syst., Int. J.*, **24**(6), 693-707. https://doi.org/10.12989/sss.2019.24.6.693

Huseynov, F., Kim, C., Obrien, E.J., Brownjohn, J.M.W., Hester, D. and Chang, K.C. (2020), "Bridge damage detection using rotation measurements - Experimental validation", *Mech. Syst. Signal Process.*, **135**, 106380. https://doi.org/10.1016/j.ymssp.2019.106380

Kok, M., Hol, J.D. and Schön, T.B. (2014), "An optimization-based approach to human body motion capture using inertial sensors", *IFAC Proceedings Volumes*, **47**(3), 79-85. https://doi.org/10.3182/20140824-6-ZA-1003.02252

Kok, M., Hol, J.D. and Schön, T.B. (2017), *Using Inertial Sensors for Position and Orientation Estimation*, Now Foundations and Trends.

Kottath, R., Narkhede, P., Kumar, V. and Karar, Vinod and Poddar, Shashi (2017), "Multiple model adaptive complementary filter for attitude estimation", *Aerosp. Sci. Technol.*, **69**, 574-581. https://doi.org/10.1016/j.ast.2017.07.011

Ladetto, Q. (2000), "On foot navigation: Continuous step calibration using both complementary recursive prediction and adaptive Kalman filtering", *Proceedings of the 13th International Technical Meeting of the Satellite Division of The Institute of Navigation* (*ION GPS 2000*), Salt Lake City, UT, USA, September.

Li, S., Wang, X., Liu, H., Zhuo, Y., Su, W. and Di, H. (2020), "Dynamic deflection monitoring of high-speed railway bridges with the optimal inclinometer sensor placement", *Smart Struct. Syst., Int. J.*, **26**(5), 591-603. https://doi.org/10.12989/sss.2020.26.5.591

Liu, C., Park, J.W., Spencer, B.F., Moon, D.S. and Fan, J. (2017), "Sensor fusion for structural tilt estimation using an acceleration-based tilt sensor and a gyroscope", *Smart Mater. Struct.*, **26**(10), 105005. https://doi.org/10.1088/1361-665X/aa84a0

Mahony, R., Hamel, T. and Pflimlin, J.M. (2008), "Nonlinear complementary filters on the special orthogonal group", *IEEE Transact. Automat. Control*, **53**(5), 1203-1218. https://doi.org/10.1109/TAC.2008.923738

Narkhede, P., Joseph Raj, A.N., Kumar, V., Karar, V. and Poddar, S. (2019), "Least square estimation-based adaptive complimentary filter for attitude estimation", *Transact. Inst. Measure. Control*, **41**(1), 235-245. https://doi.org/10.1177/0142331218755234

Narkhede, P., Poddar, S., Walambe, R., Ghinea, G. and Kotecha, K. (2021), "Cascaded complementary filter architecture for sensor fusion in attitude estimation", *Sensors*, **21**(6), 1937. https://doi.org/10.3390/s21061937

Nowicki, M., Wietrzykowski, J. and Skrzypczyński, P. (2015), "Simplicity or flexibility? Complementary Filter vs. EKF for orientation estimation on mobile devices", *Proceedings of 2015 IEEE 2nd International Conference on Cybernetics* (*CYBCONF*), Gdynia, Poland, June.

Ozioko, O., Nassar, H. and Dahiya, R. (2021), "3D printed interdigitated capacitor based tilt sensor", *IEEE Sensors J.*, **21**(23), 26252-26260. https://doi.org/10.1109/JSEN.2021.3058949

Simon, D. (2006), *Optimal State Estimation*: *Kalman*, *H Infinity*, *and Nonlinear Approaches*, John Wiley & Sons, Hoboken, New Jersey, USA.

St-Pierre, M. and Gingras, D. (2004), "Comparison between the unscented Kalman filter and the extended Kalman filter for the position estimation module of an integrated navigation information system", *Proceedings of IEEE Intelligent Vehicles Symposium*, *2004*, Parma, Italy, June.

Su, S., Li, D., Tan, N. and Li, G. (2017), "The study of a novel tilt sensor using magnetic fluid and its detection mechanism", *IEEE Sensors J.*, **17**(15), 4708-4715. https://doi.org/10.1109/JSEN.2017.2714689

Shen, Y., Fu, W., Luo, Y., Yun, C.-B., Liu, D., Yang, P., Yang, G. and Zhou, G. (2021), "Implementation of SHM system for Hangzhou East Railway Station using a wireless sensor network", *Smart Struct. Syst., Int. J.*, **27**(1), 19-33. https://doi.org/10.12989/sss.2021.27.1.019

Testoni, N., Zonzini, F., Marzani, A., Scarponi, V. and De Marchi, L. (2019), "A tilt sensor node embedding a data-fusion algorithm for vibration-based SHM", *Electronics*, **8**(1), 45. https://doi.org/10.3390/electronics8010045

BS